



Title	Autotuning of Vibrational Strong Coupling for Site-Selective Reactions
Author(s)	Hirai, Kenji; Ishikawa, Hiroto; Takahashi, Yasufumi et al.
Citation	Chemistry-A European journal, 28(47), e202201260 <a href="https://doi.org/10.1002/chem.202201260">https://doi.org/10.1002/chem.202201260</a>
Issue Date	2022-08-22
Doc URL	<a href="https://hdl.handle.net/2115/90326">https://hdl.handle.net/2115/90326</a>
Rights	This is the peer reviewed version of the following article: K. Hirai, H. Ishikawa, Y. Takahashi, J. A. Hutchison, H. Uji-i, Chem. Eur. J. 2022, 28, e202201260. , which has been published in final form at <a href="https://doi.org/10.1002/chem.202201260">https://doi.org/10.1002/chem.202201260</a> . This article may be used for non-commercial purposes in accordance with Wiley Terms and Conditions for Use of Self-Archived Versions. This article may not be enhanced, enriched or otherwise transformed into a derivative work, without express permission from Wiley or by statutory rights under applicable legislation. Copyright notices must not be removed, obscured or modified. The article must be linked to Wiley's version of record on Wiley Online Library and any embedding, framing or otherwise making available the article or pages thereof by third parties from platforms, services and websites other than Wiley Online Library must be prohibited.
Type	journal article
File Information	manuscript.pdf



# Autotuning of Vibrational Strong Coupling for Site-Selective Reactions

Kenji Hirai,<sup>\*[a], [b], [c]</sup> Hiroto Ishikawa,<sup>[c]</sup> Yasufumi Takahashi,<sup>[b], [d]</sup> James A. Hutchison<sup>[e]</sup> and Hiroshi Uji-i<sup>[a], [c], [f]</sup>

- [a] Prof. Dr. K. Hirai and Prof. Dr. H. Uji-i  
Division of Photonics and Optical Science, Research Institute for Electronic Science (RIES)  
Hokkaido University  
North 20 West 10, Kita ward, Sapporo, Hokkaido, 001-0020, Japan  
E-mail: hirai@es.hokudai.ac.jp
- [b] Prof. Dr. K. Hirai  
Precursory Research for Embryonic Science and Technology (PRESTO)  
Japan Science and Technology Agency (JST)  
4-1-8 Honcho, Kawaguchi, Saitama 332-0012, Japan.
- [c] Prof. Dr. K. Hirai, H. Ishikawa and Prof. Dr. H. Uji-i  
Division of Information Science and Technology, Graduate School of Information Science and Technology  
Hokkaido University  
North 14 West 9, Kita ward, Sapporo, Hokkaido, Japan
- [d] Prof. Dr. Y. Takahashi  
Graduate School of Engineering Electronics  
Nagoya University  
Furocho, Chikusa-ku, Nagoya-shi, Aichi 464-8603 Japan
- [e] Dr. James A. Hutchison  
School of Chemistry  
The University of Melbourne  
Masson Rd, Parkville, VIC 3052, Australia
- [f] Prof. Dr. H. Uji-i  
Department of Chemistry  
KU Leuven  
Celestijnenlaan 200F, 3001 Heverlee Leuven, Belgium

Supporting information for this article is given via a link at the end of the document.

**Abstract:** Site-selective chemistry opens new paths for the synthesis of technologically important molecules. When a reactant is placed inside a Fabry–Perot (FP) cavity, energy exchange between molecular vibrations and resonant cavity photons results in vibrational strong coupling (VSC). VSC has recently been implicated in modified chemical reactivity at specific reactive sites. However, as a reaction proceeds inside an FP cavity, the refractive index of the reaction solution changes, detuning the cavity mode away from the vibrational mode and weakening the VSC effect. Here we overcome this issue, developing actuable FP cavities to allow automated tuning of cavity mode energy to maintain maximized VSC during a reaction. As an example, the site-selective reaction of the aldehyde over the ketone in 4-acetylbenzaldehyde is achieved by automated cavity tuning to maintain optimal VSC of the ketone carbonyl stretch during the reaction. A nearly 50% improvement in site-selective reactivity is observed compared to an FP cavity with static mirrors, demonstrating the utility of actuable FP cavities as microreactors for organic chemistry.

## Introduction

As organic chemistry has developed, efforts have been focused on achieving site-selective reactions to direct syntheses towards desired compounds. To this end, chemists have fabricated a variety of catalysts with active sites that target particular functional groups. Another strategy involves sequential

protection/deprotection reactions to ensure a specific site is reactive only at a desired time. In contrast to these conventional methods, vibrational strong coupling<sup>[1]</sup> (VSC) has emerged as a new tool for site-selective reactions.<sup>[2]</sup> This requires a reaction solution be placed in an Fabry–Perot (FP) optical cavity, where specific vibrational modes of the reactants are isoenergetic with cavity photonic modes. Coupling of the collective transition dipole of the molecular vibrations with cavity vacuum fields can then drive a coherent exchange of energy, manifesting in frequency space as a splitting of the vibrational absorption band. The new absorptions are due to hybrid light-matter states, or vibropolaritons (Figure 1a).<sup>[3]</sup> Under VSC, the reactivity of the targeted functional group in a molecule can be enhanced or suppressed.<sup>[4–16]</sup> By suppressing the reactivity of a particular functional group by VSC for example, one can promote site-selective reaction at another functional group in the same molecule.

A critical issue facing practical application of site-selective VSC chemistry however is the maintenance of efficient VSC throughout the reaction. The photonic mode energy in the FP cavity depends on the separation of the cavity mirrors (Figure 1b), but also on the refractive index of the reaction mixture filling the FP cavity. Thus while for the initial reactant solution, the FP cavity mirror separation may be tuned for VSC with a target chemical bond, as the reaction progresses and the refractive index of the reaction mixture changes, detuning and loss of VSC at the target bond may occur.<sup>[6]</sup> Furthermore, since the vibrational modes of

## RESEARCH ARTICLE

similar functional groups can lie close in energy, non-targeted bonds may come into VSC with the photonic mode as the reaction progresses, further complicating the challenge of site-selective VSC chemistry.

These considerations inspired us to design an actuatable FP cavity in which the mirror separation could be automatically tuned to maintain VSC with a target vibrational mode throughout the course of a reaction. We have incorporated piezoelectric actuators onto one of the FP cavity mirrors, then using a computer-controlled feedback loop, demonstrated controlled mirror separation/approach. This allows accurate retuning of the cavity mode in response to refractive index changes within the cavity. We then applied the actuatable FP cavity to a challenging case of site-selective VSC chemistry, requiring the targeting of one of two vibrations in a single molecule that are closely-spaced energetically (Figure 1). Specifically, we demonstrate the site-selective reaction of the aldehyde over the ketone in 4-acetylbenzaldehyde within the actuatable FP cavity. The carbonyl stretching vibrations of aldehydes and ketones are excellent candidates for demonstrating the utility of our actuatable FP cavity, as their stretching modes have similar energy levels.<sup>[17]</sup> Both the aldehyde and ketone in this molecule can undergo the iodine-catalysed Prins reaction (Figure 1c).<sup>[18,19]</sup> We show here that VSC of the ketone carbonyl stretch suppresses ketone reactivity, thus selecting for aldehyde reactivity. However due to refractive index shifts during the reaction in a static FP cavity, the photonic mode detunes from the ketone carbonyl stretch and begins to couple to the aldehyde carbonyl stretch, reducing aldehyde selectivity. Using the actuatable FP cavity, and automatic tuning of the cavity mode for continuous VSC with the ketone carbonyl stretching vibration, we show a further 47% enhancement of aldehyde-selective reactivity in 4-acetylbenzaldehyde.

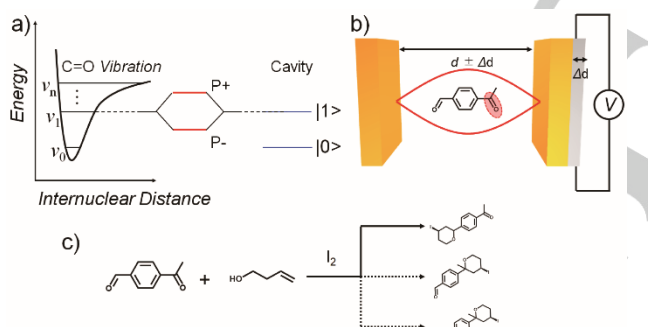


**Figure 1.** Schematic energy level diagram of vibrational strong coupling (VSC). A molecular vibrational transition ( $v_0$  to  $v_1$ ) couples to a Fabry-Perot (FP) cavity mode which contains either one ( $|1\rangle$ ) or zero ( $|0\rangle$ ) photons. The upper (P+) and lower (P-) vibropolariton branches form when there is reversible cycling of the photon between the molecular vibration and the optical cavity mode. (b) Schematic illustration of an actuatable FP cavity for site-selective reactions under VSC. The piezoelectric actuator is attached to the backside of one mirror to control the mirror separation  $d$  and therefore fix the cavity mode for VSC at a specific vibrational peak, irrespective of changes in refractive index of the reaction solution enclosed within the FP. (c) Reaction scheme of Prins cyclization. 4-acetylbenzaldehyde possesses two reactive sites (aldehyde and ketone), potentially giving three different products.

## Results and Discussion

Prior to exploring site-selective reactivity of aldehyde and ketone groups in 4-acetylbenzaldehyde, VSC was investigated for related aromatic molecules with a single reactive site, benzaldehyde (with a single aldehyde carbonyl) and acetophenone (with a single ketone carbonyl). To confirm VSC with the carbonyl stretching vibration in each case, benzaldehyde or acetophenone in 1,2-dichloroethane was placed in an FP cavity. The FP cavities consisted of 10 nm gold films as mirrors on ZnSe substrates, separated by *ca.* 10–12 microns, with the mirrors covered with a <100 nm film of silicon resin to avoid direct contact with solutions. The cavity mode was coupled to the carbonyl stretching vibration of benzaldehyde or acetophenone forming distinct new vibropolaritonic states, denoted P+ and P- (Figure 2a-d). The splitting between P+ and P- (the Rabi splitting) was  $66\text{ cm}^{-1}$  and  $55\text{ cm}^{-1}$  respectively, larger than both the carbonyl stretching vibration (FWHM  $\sim 30\text{ cm}^{-1}$ ) and the cavity mode (FWHM  $\sim 50\text{ cm}^{-1}$ ) linewidths, suggesting that strong coupling of the carbonyl stretch to the cavity vacuum field (zero-point energy of the cavity photonic mode) was achieved in each case.<sup>[20]</sup> The magnitude of the vacuum Rabi splitting energy was proportional to the square root of the concentration of benzaldehyde or acetophenone (Figure S1). Furthermore, the cavity transmission dispersions (energy vs. in-plane momentum dispersions) for the system show the typical signatures of strong coupling, with an anti-crossing of the dispersive photonic mode at the bare absorption energy of the molecular vibration (Figure S2).<sup>[3,21]</sup> Transfer Matrix Method simulations qualitatively reproduce the experimental cavity transmission dispersions,<sup>[22]</sup> with relative broadening of the experimental dispersion attributed in part to a small (<5%) variation in cavity thickness across the probed area (see Figure S2 and S3 for details).

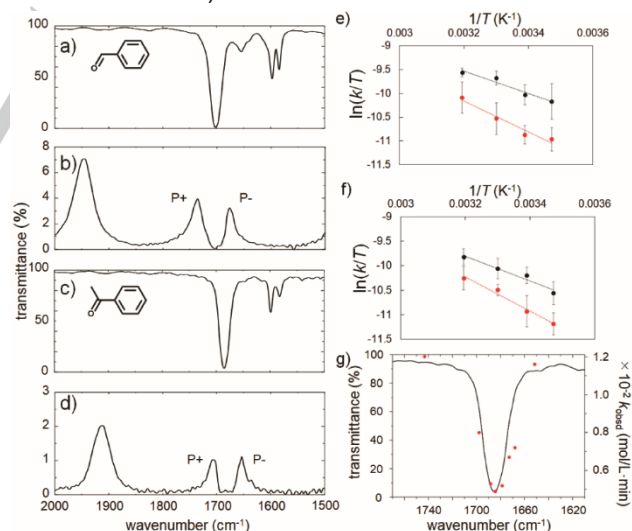


**Figure 2.** IR transmission spectra of (a) benzaldehyde, (b) a mixture of 1,2-dichloroethane and benzaldehyde in the FP cavity at normal incidence, (c) acetophenone, and (d) a mixture of 1,2-dichloroethane and acetophenone in the FP cavity at normal incidence. (e-f) Eyring plots for Prins cyclization reactions in static FP cavities for (e) benzaldehyde and (f) acetophenone. The black dots and red dots correspond to data obtained under OFF-resonance and ON-resonance conditions for the carbonyl stretch in each case. (g) The rate of Prins

## RESEARCH ARTICLE

cyclization of acetophenone as a function of static FP cavity tuning around the carbonyl stretch (red dots). The solid black line shows the IR transmission spectrum of the ketone carbonyl stretching vibration of acetophenone.

We next carried out the Prins cyclization of benzaldehyde and acetophenone in an FP cavity without a piezoelectric actuator (*i.e.*, in 'static' cavities where mirror separation is constant). There are various spectroscopic approaches to monitoring intra-cavity reaction progress, including UV-visible absorption spectroscopy of reactants/products<sup>[5,7]</sup> and infrared (IR) spectroscopy of cavity mode shifts.<sup>[2,4,6]</sup> UV-visible absorption spectroscopy is not suitable here however because of the strong absorption of iodine in UV-visible region. Thus, shifts in uncoupled IR cavity modes were used as a probe for reactive index changes during reaction progress. It should be noted that the shift of cavity modes is potentially induced by the change of mirror separation, evaporation and leaking of solvent, swelling of the spacer and temperature fluctuations.<sup>[23]</sup> To avoid these artifacts, the mirrors of the FP cavity were tightly fixed by four micron-pitched screws and sealed with chemically stable Kapton film (Figures S4-5).

The reaction kinetics of Prins cyclization of benzaldehyde and acetophenone was estimated under two conditions; namely, with the cavity mode strongly coupled with the carbonyl stretch (ON-resonance), or uncoupled (OFF-resonance). As the reaction proceeded, the refractive index of the solution in the FP cavity increased under both ON- and OFF-resonance conditions (Figure S6a), accompanied by a shift in the uncoupled cavity modes from  $\nu_0$  to  $\nu_t$  ( $\nu_t > \nu_0$ ). This shift allowed the kinetics of the Prins cyclization to be monitored using transmission spectroscopy. The plot of  $(1/c_\infty (\nu_0 - \nu_t)/(\nu_0 - \nu_\infty))$  against time was linear, indicating a second-order reaction (Figure S6b). For both benzaldehyde and acetophenone, the change in the refractive index under ON-resonance conditions was slower than that under OFF-resonance conditions (Figure S6b). This result suggests that VSC with the carbonyl stretching vibration of benzaldehyde and acetophenone suppresses their reactivity for Prins cyclization. The reaction rates under ON-resonance and OFF-resonance conditions were measured at different temperatures (15, 22, 30, and 40 °C, Table S1). At all temperatures, the reaction rates of Prins cyclization were decreased by VSC with the carbonyl stretching vibration. The reaction rates under ON-resonance conditions were slower than for OFF-resonance conditions for all temperatures. The applicability of transition state theory to VSC-modified organic reactions is under debate,<sup>[14]</sup> but the observed enthalpies and entropies of activation were estimated using Eyring plots as a comparison with previous work for Prins cyclization (Figures 2e-f). These plots suggest that activation enthalpy ( $\Delta H^\ddagger$ ) of Prins cyclization increased by approximately 8 kJ/mol under ON-resonance conditions as compared to that under OFF-resonance conditions, a 1.4-fold increase. In contrast, the activation entropy ( $\Delta S^\ddagger$ ) was not significantly altered by VSC, becoming 10% less negative (Table S2). Although the mechanism of VSC effect on chemical reactivity is not yet fully understood, the deactivation of the Prins reactions suggests the suppression of the rate-limiting step: likely the attack of alcohol group of 3-butene-1-ol to the carbonyl group or the protonation of the carbonyl group.<sup>[6, 18, 19]</sup> Similar effects of VSC on reaction rates and activation enthalpies/entropies was observed previously for Prins cyclization of acetaldehyde, propionaldehyde, cyclohexanone, and acetone.<sup>[6]</sup> In those cases,  $\Delta H^\ddagger$  increased by ~10 kJ/mol, a factor

of 1.5, and  $\Delta S^\ddagger$  became 10% less negative under VSC. Apparently, the effect of carbonyl VSC on Prins reactions is consistent across a range of simple aldehydes and ketones. The change in activation free energy from the ON- to OFF-resonance ( $\Delta\Delta G^\ddagger_{\text{ON-OFF}}$ ) was estimated to be 1.8 and 1.6 kJ/mol for benzaldehyde and acetophenone, respectively.  $\Delta\Delta G^\ddagger_{\text{ON-OFF}}$  is much smaller than the change of  $\Delta H^\ddagger$  of ~8 kJ/mol for each case. Similar observations were made recently for the VSC-modified reaction of p-nitrophenylbenzoate with tetrabutylammonium fluoride.<sup>[24]</sup> There, the VSC-induced change in reactivity of p-nitrophenylbenzoate was attributed to the reshuffling of electron density locally at the reaction center. Since reactivity in Prins cyclization relies on the nucleophilic attack at a carbonyl carbon,<sup>[6]</sup> reshuffling of electron density (bond polarity) also results in changing reactivity, and we previously discussed VSC-induced changes in carbonyl bond polarity as a possible driver of the VSC effect on Prins reactions. Thus common mechanistic features may be emerging here, even though the Prins cyclization is decelerated under VSC of the carbonyl stretch, while the reaction of p-nitrophenylbenzoate is accelerated. The opposite directions of VSC-induced effects may be due to different reaction mechanisms or the role of solvent molecules in the p-nitrophenylbenzoate reaction.

To clarify the significance of cavity mode tuning, the reaction rate was measured for various static cavity mirror separations, scanning the optical mode around the carbonyl stretch energy of acetophenone (Figure 2g). The effect of VSC on the reaction rate clearly depends on the degree of resonance, with the rate of reaction as a function of cavity mode energy (red dots) being superimposable on the shape of carbonyl stretching vibration band (black line). When the cavity mode was adjusted to match the maximum of the carbonyl stretch, the reaction rate was decreased by 60 % compared to the completely detuned case. This result indicates that VSC of the carbonyl stretch is the dominant modifier of Prins cyclization reactivity, even if other stretches (e.g. OH stretches) may fall in resonance with cavity modes in other spectral regions. With respect to 4-acetylbenzaldehyde, these results suggest that the cavity mode should be adjusted to the absorption maximum of the ketone throughout the reaction to realize the most efficient selective reactivity of aldehyde.

Subsequently, VSC of the carbonyl stretches of 4-acetylbenzaldehyde in the FP cavity was investigated. The carbonyl stretching vibrations of the aldehyde and ketone in 4-acetylbenzaldehyde were observed at 1706 and 1687  $\text{cm}^{-1}$ , respectively (Figure 3a). The mirror separation was adjusted to 12.3 microns such that, at normal incidence ( $k_x = 0 \mu\text{m}^{-1}$ ) the cavity mode is tuned to the ketone carbonyl stretch (1687  $\text{cm}^{-1}$ ). As the incidence angle is increased, the cavity mode moves through resonance with the aldehyde stretch. Being closer in energy than the cavity photon linewidth, both vibrational modes couple simultaneously to the cavity photon, resulting in three polariton branches; called here the upper (UP), middle (MP) and lower (LP) polariton branches. The experimental cavity transmission dispersion shows distinct UP and LP branches above and below the anti-crossing at the carbonyl stretch absorption dips at 1706 and 1687  $\text{cm}^{-1}$  (Figure 3b). The MP branch sits between the two vibrations at 1700  $\text{cm}^{-1}$  but is heavily damped and barely visible. The same features are qualitatively reproduced in the simulated transmission dispersion (Figure 3c).

## RESEARCH ARTICLE

A multimode coupled oscillator model (COM) fit was performed assuming the simultaneous interaction of the ketone carbonyl stretch (with energy  $E_{Ex1}$ ) and the aldehyde carbonyl stretch (with energy  $E_{Ex2}$ ) with the 6th FP cavity mode (with energy  $E_{cav}^{6th}$ ), for which the appropriate Hopfield matrix is:

$$\begin{pmatrix} E_{cav}^{6th} & \hbar\Omega_1/2 & \hbar\Omega_2/2 \\ \hbar\Omega_1/2 & E_{Ex1} & 0 \\ \hbar\Omega_2/2 & 0 & E_{Ex2} \end{pmatrix}$$

The three resulting eigenstates are plotted in white dashed lines in Fig. 3c assuming equal interaction energies for each cavity mode-vibration interaction ( $\hbar\Omega_1/2 = \hbar\Omega_2/2 = 26 \text{ cm}^{-1}$ ), and with the bare cavity mode energies extracted from TMM simulations for the 12.3 microns mirror cavity filled with a flat background refractive index of 1.445. The eigenvector decomposition (Hopfield coefficients) indicates that, at normal incidence ( $k_x = 0 \text{ } \mu\text{m}^{-1}$ ), the LP branch is 55% photonic, 32% ketone carbonyl stretch, and 13% aldehyde carbonyl stretch.

We next studied Prins cyclization of 4-acetylbenzaldehyde with VSC of the carbonyl stretches to improve site-selective reactivity between the aldehyde and ketone groups. The aldehyde and ketone of 4-acetylbenzaldehyde are both reactive for Prins cyclization. In free solution, the % reaction ratio of the aldehyde:ketone is 60%, as calculated from the decrease in the IR peak intensities of the aldehyde and ketone after 30 minutes reaction time (Figure S7).

Prins cyclization of 4-acetylbenzaldehyde was then carried out in a static cavity, with the cavity mode tuned to the absorption maximum of the ketone carbonyl stretch at normal incidence at the beginning of the reaction (note, as discussed earlier this optical resonance position will drift as the reaction proceeds due to refractive index changes and static mirror positions). The reaction ratio aldehyde:ketone was again calculated from IR spectroscopy after 30 minutes (the reaction solution was removed from cavity with a syringe).

Under initial ON-resonance conditions of the static cavity with the ketone, the reaction ratio aldehyde:ketone increased owing to the reactivity of the ketone being suppressed, reaching  $79 \pm 4\%$  (higher than a 60% ratio observed in free solution). As shown in Figure 3d, the aldehyde selectivity increase depends smoothly on the degree of resonance with the ketone from 1650 to 1690  $\text{cm}^{-1}$ , with aldehyde:ketone reaction ratio plotted as a function of the initial cavity mode energy (blue dots) being superimposable on the carbonyl stretching band of the ketone of 4-acetylbenzaldehyde (right-hand peak of the black curve). The aldehyde:ketone reaction ratio then goes down again when the resonance moves into the aldehyde carbonyl stretch region ( $>1700 \text{ cm}^{-1}$ ). When the cavity mode was adjusted to be completely detuned, the aldehyde:ketone reaction ratio was reduced to  $57 \pm 4\%$ , similar to the free solution case of 60%. On the other hand, when the cavity mode was adjusted to be initially at the carbonyl stretching band of the aldehyde, the reaction ratio of the aldehyde:ketone decreased further to  $53 \pm 3\%$ . These results confirm that by using a static FP cavity to drive VSC of the carbonyl stretches in 4-acetylbenzaldehyde, one can effectively control relative reactivity of the ketone and aldehyde compared to free solution. Specifically, aldehyde selectivity can be increased by 32% when initially tuning the static cavity to the ketone carbonyl, or reduced by 12% when initially tuning the static cavity to the aldehyde carbonyl.

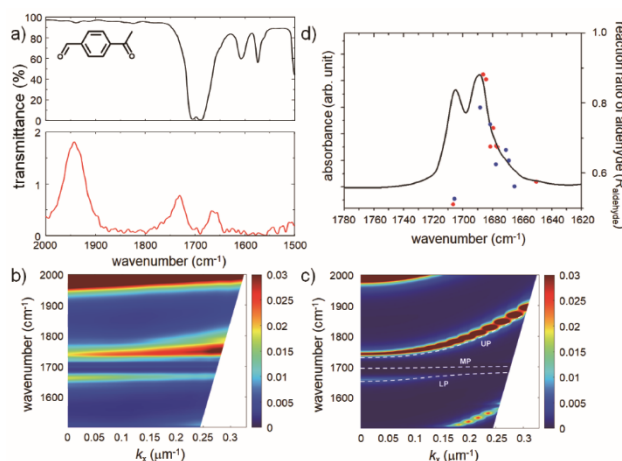


**Figure 3.** (a) IR transmission spectra of 4-acetylbenzaldehyde (black) and 4-acetylbenzaldehyde with 1,2-dichloroethane in a FP cavity at normal incidence (red). The 6th cavity mode is coupled to the carbonyl stretching vibration of the ketone at  $1687 \text{ cm}^{-1}$ . (b) Angular dispersion of transmittance of 4-acetylbenzaldehyde/1,2-dichloroethane in an FP cavity. (c) Theoretical dispersion of 4-benzaldehyde/1,2-dichloroethane in an FP cavity. The upper polariton, middle polariton and lower polariton branches predicted from a coupled oscillator model are indicated by white dashed lines. (d) Ratio of aldehyde:ketone carbonyl reactivity for 4-acetylbenzaldehyde as a function of FP cavity tuning for a static cavity (blue dots, indicating cavity mode energy at the beginning of the reaction, however as mirror separation is kept constant, this energy will shift during the reaction) and for an actuatable FP cavity (red dots, these cavity mode energies are kept constant through the reaction by tuning mirror separation). The solid black line shows the aldehyde (left peak, maximum at  $1706 \text{ cm}^{-1}$ ) and ketone (right peak, maximum at  $1687 \text{ cm}^{-1}$ ) stretching vibrations of 4-acetylbenzaldehyde.

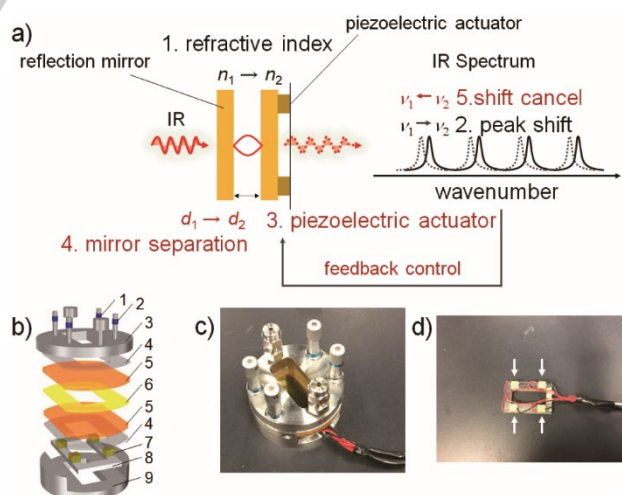


**Figure 4.** (a) System for controlling the cavity modes: 1. The refractive index changes from  $n_1$  to  $n_2$  as the reaction proceeds. 2. The cavity peaks shift because of the change in refractive index. Once a peak shift is detected, the feedback system starts. The displacement of piezoelectric actuators is calculated based on eq.4 in Supporting Information. 3. Piezoelectric actuators

## RESEARCH ARTICLE

contract or expand. 4. The mirror separation is changed by the contraction/expansion of the piezoelectric actuators. 5. The peak shift is cancelled by the change in mirror separation. (b) Schematic illustration of the FP cavity with piezoelectric actuators: 1. Inlet of the reaction solution, 2. Micrometer-pitched screw, 3. Stainless steel lid, 4. Teflon film, 5. Au sputtered on ZnSe, 6. Kapton film, 7. Piezoelectric actuator, 8. Stainless steel stage for the piezoelectric actuator, 9. Stainless steel stage. The two reflective mirrors (5) are parallel and facing each other, separated by a spacer film (6). The piezoelectric actuators (7) are attached to the backside of one of the mirrors. These components are assembled, and the reaction solution is introduced between the reflective mirrors. (c,d) Photographs of the FP cavity with piezoelectric actuators. The white arrows indicate the piezoelectric actuators, which are connected to the data acquisition system.

However, taking the case of tuning to the ketone vibration of 4-acetylbenzaldehyde, during the 30-minute reaction the cavity resonance peak shifts (in the absence of interactions with molecular vibrations) from  $1687\text{ cm}^{-1}$  to  $1718\text{ cm}^{-1}$ , due to refractive index changes associated with reactant consumption and product formation. This means that the cavity mode is progressively detuned from the energy of the ketone carbonyl ( $1687\text{ cm}^{-1}$ ), and progressively passes through the energy of the aldehyde carbonyl ( $1706\text{ cm}^{-1}$ ) during the reaction. This dilutes the selective suppressive effect of VSC at the ketone.

To improve site-selective reactivity of 4-acetylbenzaldehyde, piezoelectric actuators associated with a feedback program were installed in the FP cavity (Figures 4 and S8), allowing tuning of mirror separation and thus optical cavity mode energies with  $0.5\text{ cm}^{-1}$  resolution with ease. For 4-acetylbenzaldehyde reactions inside these actuatable cavities, uncoupled cavity modes were monitored every 5 seconds of the reaction and the mirror separation was re-tuned to compensate for any shifts due to refractive index changes, thus maintaining the cavity mode at the desired energy throughout the reaction (Figure S9). For the case of VSC of the ketone stretching band, the actuatable FP cavity with automated cavity mode tuning should allow continuous suppression of the ketone reactivity through the reaction and thus optimized aldehyde reactivity.

The results of this experiment are shown in Figure 3d (red dots). Using an actuatable FP cavity to maintain perfect ON-resonance conditions at the ketone stretch of 4-acetylbenzaldehyde throughout the reaction, the aldehyde:ketone reaction ratio increased to  $88\pm 3\%$  compared to  $58\pm 3\%$  for the completely detuned case. Again, the actuatable FP cavity VSC effects depend on the degree of resonance, with the aldehyde selectivity as a function of cavity mode energy (red dots) being superimposable on the carbonyl stretching band of the ketone of 4-acetylbenzaldehyde (right-hand peak of the black curve). When the cavity mode was maintained at the aldehyde carbonyl stretch energy, the aldehyde:ketone reaction ratio decreased to  $52\pm 3\%$  (Figure 3d). Thus, in the actuated FP cavity, aldehyde selectivity can be increased by 47% when tuning to the ketone carbonyl, or reduced by 15% when tuning to the aldehyde carbonyl, compared to free solution. The increase of aldehyde:ketone reaction ratio by actuated FP cavity compared to the static one is larger than the standard errors.

Overall, the actuated FP cavity improves cavity-enhanced aldehyde selectivity by 47% (47% vs 32% cavity-enhanced selectivity for actuated and static FP cavities respectively) when targeting the ketone carbonyl of 4-acetylbenzaldehyde. Again, this is attributed to the maintenance of the cavity mode at the ketone stretch energy throughout the reaction, and thus maintenance of optimized reaction suppression despite reaction solution refractive index changes. Targeting the aldehyde stretch for VSC with the actuatable FP cavity probably enhances suppression of its reactivity in 4-acetylbenzaldehyde (15% vs 11% cavity-enhanced aldehyde suppression for actuated and static FP cavities respectively) but the differences are close to experimental uncertainty ( $\pm 2\%$ ).

## Conclusion

In summary, we have developed actuatable FP cavities allowing the cancelling of temporal shifts of their cavity modes due to chemical reaction-induced refractive index changes in enclosed solutions. We then showed that these actuatable FP cavities can enhance the site-selective VSC-modified chemistry by nearly 50% in a specific challenging case.

As seen here for the case of selective reactivity of the aldehyde or ketone during Prins cyclization of 4-acetylbenzaldehyde, even when the maxima of the respective reactive carbonyl stretches are energetically close such that their bands overlap, adjusting the cavity mode to the peak of either vibration at normal incidence has a significant influence on VSC-modified reaction kinetics. This matches control experiments on VSC-modified Prins cyclization of benzaldehyde and acetophenone, with suppressive effects observed in both cases. It also matches previous observations that the resonant mode at normal incidence largely contributes to modulation of reaction kinetics.<sup>[2,4-6]</sup> Importantly here, it suggests that even small shifts in cavity modes associated with refractive index changes during reactions cannot be ignored if VSC-modified chemistry mechanisms are to be clearly elucidated and efficiencies maximized.

Indeed, selectivity for aldehyde reactivity in Prins cyclization of 4-acetylbenzaldehyde could be improved by nearly 50% by autotuning the cavity mode to remain at the peak of the ketone throughout the reaction, even though the vibrational modes of the ketone and aldehyde sit within  $20\text{ cm}^{-1}$  of each other. This is the first example of such extremely precise site-selective VSC chemistry for vibrational modes with similar energy levels maintained over the course of a reaction and is one step along the path to developing microcavity reactors for practical molecular chemistry using cavity vacuum fields.

## Experimental Section

**FP Cavity:** An FP cavity cell with fine-pitched microscrews was purchased from TTC Inc., Japan. Kapton films with a thickness of  $5\text{ }\mu\text{m}$  were purchased from Du Pont-Toray Co., Ltd. ZnSe windows were purchased from Specac Ltd., UK. Au with a thickness of  $10\text{ nm}$  was coated on the ZnSe windows by sputtering. The silicon resin solution was spin-coated on top of the Au layer, followed by drying in an oven. The FP cavity is reusable after washing out the reaction solutions.

**Reaction Conditions for Benzaldehyde or Acetophenone:** I<sub>2</sub> (25.4 mg, 0.1 mmol) was dissolved in 1,2-dichloroethane (500  $\mu$ L). Benzaldehyde (1.2 mmol) or acetophenone (1.2 mmol) and 3-butene-1-ol (1.2 mmol) were added to the resultant solution. The cavity of the FP cell was filled with the obtained solution and the temperature was controlled at 15, 22, 30, or 40 °C.

**Reaction Conditions for 4-Acetylbenzaldehyde:** I<sub>2</sub> (50.8 mg, 0.2 mmol) was dissolved in 1,2-dichloroethane (1 mL). 4-Acetylbenzaldehyde (17.8 mg, 0.12 mmol) and 3-butene-1-ol (0.24 mmol) were added to the resultant solution. The cavity was filled with the obtained solution and the temperature was controlled at 22 °C.

**Piezoelectric Actuator:** Piezoelectric actuators (PA4FKW, Thorlab) were attached to the backside of the reflection mirror (Figure 4). The expansion and contraction of the piezoelectric actuators were controlled using a piezoelectric driver (PH103, THK Precision Co., Ltd.) connected to a data acquisition system (USB-6002, National Instruments Corporation). The control program for the piezoelectric actuators was written using LabView.

## Acknowledgements

This work was supported by JST PRESTO (JPMJPR18TA), the New Chemical Technology Research Encouragement Award 2020, and JSPS KAKENHI (JP18K19085, JP21H01899) to K.H., and partially supported by the JSPS Core-to-Core Program A. Advanced Research Networks to H.U. and JST PRESTO (JPMJPR18T8) to Y.T. J.A.H. acknowledges an Australian Research Council (ARC) Future Fellowship award (FT180100295). K.H., H.U. and J.A.H. acknowledge the Study Melbourne Research Partnerships program made possible by funding from the Victorian Government through Study Melbourne.

## Conflict of Interest

The authors declare no conflict of interest.

## Data Availability Statement

The data that support the findings of this study are available in the supplementary material of this article.

**Keywords:** Vibrational Strong Coupling • Fabry-Perot Cavity, Prins Reactions • Piezoelectric Actuators • Infrared Spectroscopy

## References

- [1] J. F. Garcia-Vidal, C. Ciuti, C. and T. W. Ebbesen, *Science* **2021**, 373, eabd0336.
- [2] A. Thomas, L. Lethuillier-Karl, K. Nagarajan, R. M. A. Vergauwe, J. George, T. Chervy, A. Shalabney, E. Devaux, C. Genet, J. Moran, T. W. Ebbesen, *Science* **2019**, 363, 615–619.
- [3] A. Shalabney, J. George, J. Hutchison, G. Pupillo, C. Genet, T. W. Ebbesen, *Nat. Commun.* **2015**, 6, 5981.
- [4] A. Thomas, J. George, A. Shalabney, M. Dryzhakov, S. J. Varma, J. Moran, T. Chervy, X. Zhong, E. Devaux, C. Genet, J. A. Hutchison, T. W. Ebbesen, *Angew. Chem. Int. Ed.* **2016**, 55, 11462–11466.
- [5] R. Vergauwe, A. Thomas, K. Nagarajan, J. George, T. Chervy, M. Seidel, E. Devaux, V. Torbeev, T. W. Ebbesen, *Angew. Chem. Int. Ed.* **2019**, 58, 15324–15328.
- [6] K. Hirai, R. Takeda, J. A. Hutchison, H. Uji-i, *Angew. Chem. Int. Ed.* **2020**, 59, 5332–5335.
- [7] J. Lather, P. Bhatt, A. Thomas, T. W. Ebbesen, J. George, *Angew. Chem. Int. Ed.* **2019**, 58, 10635–10638.
- [8] A. Sau, K. Nagarajan, B. Patraha, L. Lethuillier-Karl, R. M. A. Vergauwe, A. Thomas, J. Moran, C. Genet, T. W. Ebbesen, *Angew. Chem. Int. Ed.* **2021**, 60, 5712–5717.
- [9] J. Lather, J. George, *J. Phys. Chem. Lett.* **2021**, 12, 379–384.
- [10] M. Du, J. Yuen-Zhou, *Phys. Rev. Lett.* **2022**, 128, 09601.
- [11] J. F. Triana, F. J. Hernández, F. Herrera, *J. Chem. Phys.* **2020**, 152, 234111.
- [12] J. Galego, C. Climent, F. J. Garcia-Vidal, J. Feist, *Phys. Rev. X* **2019**, 9, 021057.
- [13] X. Li, A. Mandal, P. Huo, *Nat. Commun.* **2021**, 12, 1315.
- [14] C. Schäfer, J. Flick, E. Ronca, P. Narang, A. Rubio, arXiv:2104.12429v3
- [15] K. Nagarajan, A. Thomas, T. W. Ebbesen, *J. Am. Chem. Soc.* **2021**, 143, 16877–19889.
- [16] K. Hirai, J. A. Hutchison, H. Uji-i, *ChemPlusChem* **2020**, 85, 1981–1988.
- [17] C. Lievens, D. Mourant, M. He, R. Gunawan, X. Li, C. Z. Li, *Fuel* **2011**, 90, 3417–3423.
- [18] J. S. Yadav, B. V. Subba Reddy, V. H. Krishna, T. Swamy, G. G. K. S. Narayana Kumar, *Can. J. Chem.* **2007**, 85, 412–415.
- [19] J. S. Yadav, B. V. Subba Reddy, G. G. K. S. Narayana Kumar, T. Swamy, *Tetrahedron Lett.* **2007**, 48, 2205–2208.
- [20] T. W. Ebbesen, *Acc. Chem. Res.* **2016**, 49, 2403–2412.
- [21] J. George, T. Chervy, A. Shalabney, E. Devaux, H. Hiura, C. Genet, T. W. Ebbesen, *Phys. Rev. Lett.* **2016**, 117, 153601.
- [22] K. Hirai, H. Ishikawa, T. Chervy, J. A. Hutchison, H. Uji-i, *Chem. Sci.* **2021**, 12, 11986–11994.
- [23] B. S. Simpkins, A. D. Dunkelberger, J. C. Owrutsky, *J. Phys. Chem. C* **2021**, 125, 19081–19087.
- [24] J. Lather, A. N. K. Thabassum, J. Singh, J. George, *Chem. Sci.*, **2022**, 13, 195–202

